Metallomics

Accepted Manuscript

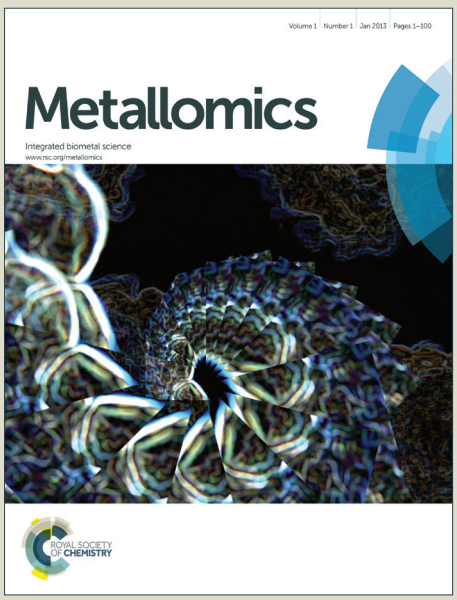

ROYAL SOCIETY OF CHEMISTRY

www.rsc.org/metallomics

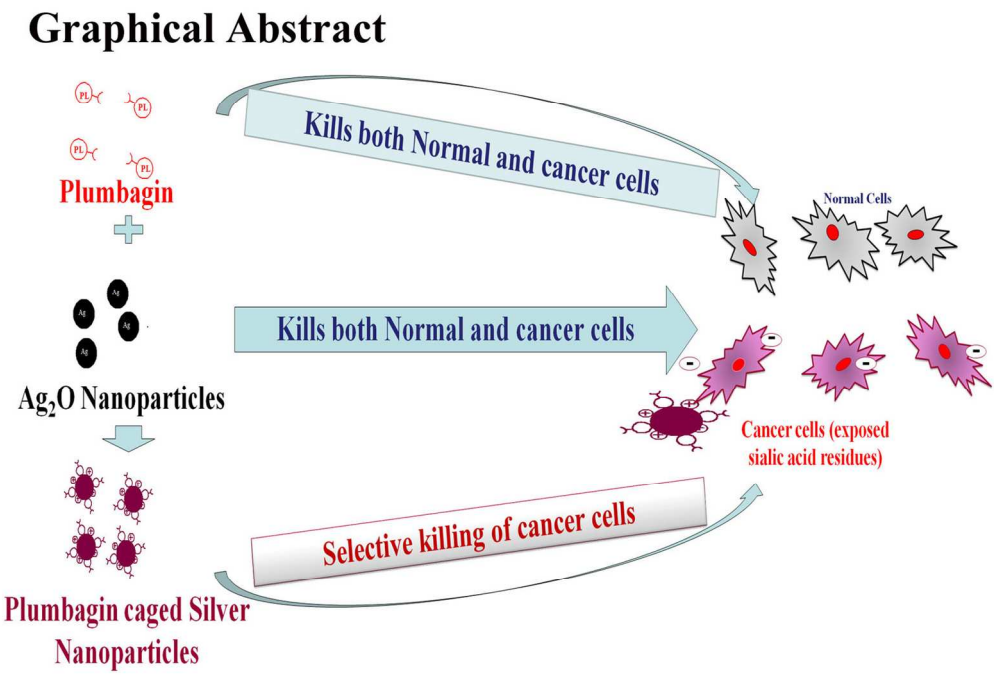

Graphical Abstract
589x392mm (72 x 72 DPI)

Journal Name

RSCPublishing

ARTICLE

Caging of plumbagin on silver nanoparticles imparts selectivity and sensitivity to plumbagin for targeted cancer cell apoptosis

Cite this: DOI: 10.1039/x0xx00000x

Received 00th January 2012,
Accepted 00th January 2012

DOI: 10.1039/x0xx00000x

www.rsc.org/

N. Duraipandy [a,b], Rachita Lakra[a], Srivatsan Kunnavakkam Vinjimur[a], Debasis Samanta[a], Purna Sai K [a,b] and Manikantan Syamala Kiran [a,b*]

Plumbagin is a nutraceutical with potent anti-cancer activity. However, the therapeutic efficacy of plumbagin is overshadowed by lack of sensitivity and selectivity towards cancer cells. The present study evaluated the use of nano-biotechnological intervention to cage plumbagin on silver nanoparticles for selective targeting of its biological effects towards cancerous cells. Caging of plumbagin on silver nanoparticles imparted selectivity and sensitivity to plumbagin for selective killing of cancer cells by altering the redox signalling events in the cancer cells. The selectivity and sensitivity of plumbagin towards cancer cells was due to the cumulative expression of the properties of plumbagin and nanoparticles which specifically affected the differential cancer cell microenvironment by altering the pyruvate kinase activity that regulates the ROS challenge in cancerous cells. The positive surface charge of plumbagin caged silver nanoparticle (PCSN) aide in getting them targeted towards anionic cancerous cells due to the exposed terminal carboxyl group of sialic acid residues. Further we observed that the effective concentration to induce apoptosis was brought down to 50% on caging of plumbagin on silver nanoparticles. We observed no such effect with individual compound alone. The results indicated that the physico-chemical and biochemical properties of plumbagin significantly changed after conjugation with nanomaterial that facilitated "adding-in" therapeutical values to plumbagin which would otherwise be overshadowed by its lack of sensitivity and selectivity against cancer cells.

Introduction

Nutraceuticals are gaining much current attention due to their various therapeutic effects.[1] Several research reports indicate that they are biocompatible and exhibit no or little harmful side effects.[2,3] Unfortunately, some of the nutraceuticals that have potent therapeutic effects are overshadowed by their toxic effect on normal cells.[4-6] One such nutraceutical with potent biological effect that can be explored as therapeutic molecule is plumbagin but it has been reported to be non-selective and non-specific against diseased cells which makes it difficult to formulate plumbagin as a therapeutic agent.[7] Plumbagin (2-methyl-5-hydroxy-1, 4-naphthoquinone) is a naturally occurring yellow pigment, produced by members of Plumbaginaceae, accumulated mostly in roots.[8] It exhibits assorted pharmacological effect mainly antibacterial, antiatherosclerotic and is a well-known agonist of tumourigenesis.[9-11] Plumbagin could be developed as potent therapeutic agents if selectivity and sensitivity of its biological effects could be targeted against the diseased cells. However such limitations could be overcome either by identification of functional target molecule of nutraceuticals on the cell or modify the activity of nutraceuticals to reduce their toxicity and impart selectivity.[12,13] Currently many research attempts are being made to impart selectivity and sensitivity to nutraceuticals against diseased cells. One such mechanism includes conjugation of this nutraceuticals with other compounds such as nanomaterials which would results in good physico-chemical and biochemical effects. [14, 15]

Numerous reports are also available that demonstrate the therapeutic potential of crude extract of plant and animal origin showing little or no effect when the active compound from that extract is used alone. Several research works are directed toward conjugating molecules for better biological and physico-chemical effects.[16] Conjugation enables the modification of the properties of both nutraceuticals as well as conjugate moiety (nanoparticles).[17] The activity and the physicochemical properties of the nutraceuticals and conjugate molecules significantly change after conjugation owing to the cumulative physico-chemical properties of both the nutraceuticals and the nanoparticles.[18] Further, various parameters such as shape, surface aggregation/disaggregation properties are also influenced by the size reduction to nano level in addition to

enhanced surface area aided covalent interactions.[19,20] The conjugation of nanoparticle also facilitates the reduction of surface energy with simultaneous enhancement of their functionality and stability through a protective coating preventing nanoparticle agglomeration.[21] Furthermore this also reduces the toxicity of active compound to some extent. In the present study we analyzed the effect of conjugation of plumbagin on silver nanoparticle and studied its effect on the biological activities of plumbagin. We observed that the biochemical activities of plumbagin drastically changed after conjugation. Many of the side effects of plumbagin were overcome on conjugation with silver nanoparticles.

Experimental

All the biochemicals and chemicals used for this study were of analytical grade from M/S Sigma Aldrich. HaCaT (immortalized human keratinocytes), A431 (epidermoid carcinoma cell lines) NIH3T3 and MG63 cells were purchased from NCCS Pune India. All the tissue culture wares were from M/s Nunc, Denmark.

Characterization of plumbagin caged silver nanoparticles
The UV-visible spectrum of nanoparticles was acquired by dispersing the nanoparticles in deionised water and the spectral changes was analyzed using Perklin Elmer UV spectrophotometer. The dispersity and particle size was measured by Photo Correlation Spectroscopy (PCS) using Zetasizer 3000HS (Malvern Instruments Ltd., UK). Theta potential of silver crystals was measured by X-ray diffractometer (XRD). The conjugation of plumbagin on silver nanoparticle was identified using Fourier transform- Infra Red (FT-IR) spectroscopy, Scanning Electron Microscopy (SEM) combined with Energy Dispersive X-RAY spectroscopy (EDS) and Transmission Electron Microscopic (TEM) techniques.

Quantitation of plumbagin caging on silver nanoparticle:
In order to determine the amount of incorporation of plumbagin on the silver nanoparticles, the PCSN were treated with 0.5M alcoholic KOH to solubilise the nutraceuticals. The solubilised plumbagin was collected by simple centrifugation and subjected to estimation against plumbagin standards colorimetrically. The following formula was used to calculate the drug loading amount.
Drug incorporation amount = O.D of Test × Conc. of Standard/ O.D of standard × Vol. of Test

Mitochondrial Dehydrogenase assay:
To investigate the cytotoxic effect of plumbagin caged silver nanoparticle, the mitochondrial dehydrogenase activity was measured by using 3-(4, 5-dimethylthiazolyl-2)-2, 5-diphenyltetrazolium bromide (MTT) salts.[22] MTT assay was performed using HaCaT and A431 cells. Cells (approximately 15000) were treated with plumbagin caged silver nanoparticles at varying concentrations (1.25, 2.5 and 5µM respectively). After 24 hrs incubation the cells were incubated with MTT solution (0.5mg/ml) for 4 hrs at 37°C. After 4 hrs, blue/purple formazan crystals formed were solubilised by DMSO and the absorbance was read at 570 nm in Bio-Rad Elisa plate reader.

In situ phosphatidyl serine (PS) externalization assay:
The effect of plumbagin caged silver nanoparticles on apoptosis in HaCaT and A431 cells were analysed by performing Annexin propidium iodide staining. Briefly, HaCaT and A431 cells were treated with varying concentrations (1.25, 2.5 and 5 µM) of plumbagin caged silver nanoparticles and incubated in a CO_2 incubator for 6 hrs. After incubation the cells were washed with PBS followed by staining with TACS Annexin V-FITC Apoptosis Detection Kit (catalogue number 4830-250-K) following the manufacturer's (M/s. Trevigen Inc, MD, USA) instructions. The images of the cells were captured using Leica fluorescent microscope.

Estimation of reactive oxygen species (ROS) generation:
To determine the ROS generation, A431 and HaCaT cells were treated with varying concentrations of plumbagin caged silver nanoparticle (1.25, 2.5 and 5 µM respectively). After 6 hrs incubation, the cells were washed and re-suspended in phosphate-buffered solution and incubated with 5µM- dichloro dihydrofluorescin diacetate (DCFH-DA) in PBS for 30 minutes in the dark. [23] After incubation the images of the cells were taken with blue filter (495 nm excitation and 523 nm emission) using Leica fluorescent microscope.

Caspase assay:
The caspase activity was measured using caspase 3 and 9 colorimetric assay kit from R&D system as per manufacturer's instructions. Briefly, Normal and cancer cells were treated with various concentrations of the nanoparticle and incubated for 6 hrs. After incubation these cells were lysed to collect their intracellular contents. The cell lysate was tested for protease activity by treating it to caspase-specific peptide that is conjugated to the colour reporter molecule p-nitro aniline (pNA) and the activity was detected by the amount of proteolytic cleavage of chromophore pNA, which was measured at 405 nm in Bio-Rad Elisa plate reader.

Pyruvate Kinase (PK) Assay:
The activity of pyruvate kinase enzyme was measured by NADH/Lactate Dehydrogenase coupled assay. Briefly cells were treated with various concentrations of plumbagin and plumbagin caged silver nanoparticles and maintained in culture for 12 hrs in a CO_2 incubator at 95% air and 5% CO2 atmosphere. The cells were collected after incubation, washed in ice cold PBS and lysed in lysis buffer containing 50mM Tris pH 7.5, 1mM EDTA, 150mM NaCl, 1% NP-40, 1 mM dithiothreitol and protease inhibitors.[24] These cell lysates provided the substrate for the assay and PK activity was estimated by measuring the decrease in the absorbance due to the oxidation of NADH to NAD^+ at 340nm in double beam UV absorption spectrophotometer. The reaction was started by adding protein normalised cell lysate to the reaction mixture (50 mM Tris (pH 7.5), 100 mM KCl, 5 mM $MgCl_2$, 1.25 mM ADP, 0.5 mM PEP, 0.28 mM NADH and 8 units of LDH). The activity of PK enzyme was expressed in OD units /mg protein.

Results and Discussion

Synthesis and characterization of plumbagin caged silver nanoparticles

Plumbagin caged silver nanoparticles were prepared by oxido-reduction method using plumbagin and silver as the precursor. 10mM of silver nitrate solution in sterile double distilled water was reacted with final concentration 10mM of Plumbagin dissolved in 0.5M KOH at RT. 0.5M KOH (without plumbagin) alone served as control. Nanoparticles were collected by centrifugation at 8500rpm for 10 minutes. Nanoparticles were freeze dried using a lyophilizer

to attain the fine structures of particles. The lyophilized nanoparticles were characterized by UV-Visible spectroscopy, FT-IR, XRD, PCS, SEM and TEM techniques. Potassium hydroxide reacts with silver nitrate to form silver hydroxide which being highly unstable forms Ag_2O nanoparticles. But in the presence of plumbagin the silver hydroxide gets converted into silver plumbagin complex wherein the colorless silver solution turns into a dark precipitate. The reaction mechanism of silver plumbagin nano-conjugates formation is given below

Control Nanoparticles:-

$2AgNO_3 + 2KOH \rightarrow [AgOH] \rightarrow Ag_2O+2KNO_3$

[Highly Unstable]

In presence of Plumbagin:-

$2AgNO_3 + 2KOH \rightarrow 2[AgOH] + 2C_{11}H_8O_3 \rightarrow 2C_{11}H_7O_3\,Ag + 2H_2O + 2KNO_3$

The nanoparticles were characterized by UV-Visible spectroscopy. Fig.1a shows the UV spectra of plumbagin caged silver nanoparticle.

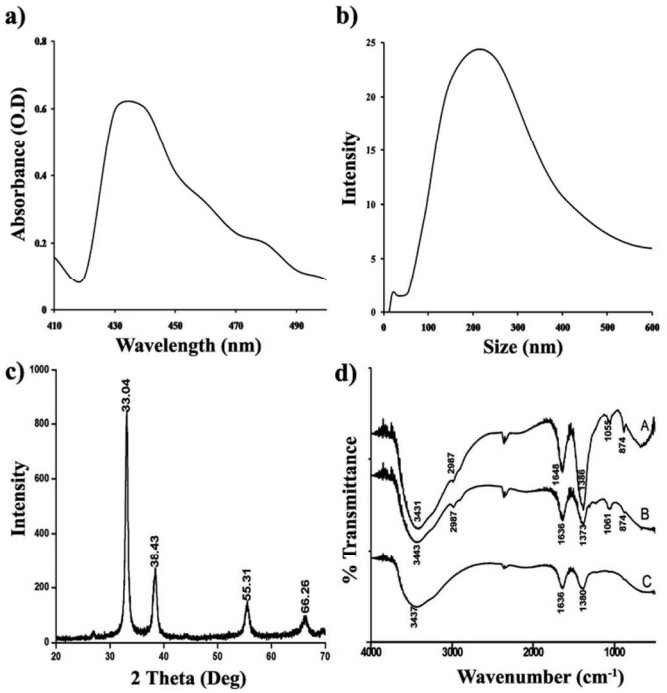

Fig.1 Characterization of plumbagin caged silver nanoparticles a) UV-visible spectrum of plumbagin caged silver nanoparticles b) Particle size analysis of plumbagin caged silver nanoparticles. c) XRD pattern of plumbagin caged silver nanoparticles. d) FTIR spectra of Plumbagin (A), Plumbagin solubilized from plumbagin caged silver nanoparticles (B), plumbagin caged silver nanoparticles (C). The FTIR spectrum shows conjugation of plumbagin on silver nanoparticles as indicated by similar FTIR patterns for plumbagin in all the samples analyzed.

The absorbance maximum was observed at around 430 nm. The conjugation of nutraceuticals on to silver nanoparticle was analyzed based on the presence of the functional group on the surface of nanoparticle by FT-IR spectroscopy. Fig.1d shows the FT-IR spectrum of plumbagin standard (A), plumbagin solubilised from silver nanoparticle (B) and plumbagin caged silver nanoparticles (C). The wave number having broad bands of 3431, 3443, 3437 (OH or phenol stretching); 1636, 1648 (amide C=O stretching); 1380, 1373, 1386 (CH3) was observed in all the three groups (A, B, and C) that indicated the presence of plumbagin moieties on silver nanoparticles. Further the conjugation of plumbagin on silver nanoparticles was also confirmed by the disappearance of the peaks having the wave number 2987 (O-H, stretching vibration) and 1061, 1056 (C-O) in the spectrum of plumbagin caged nanoparticle (C). We assume that the disappearance of these bands may be due to the involvement of these groups for conjugation of plumbagin on silver nanoparticles. Thus observation of similar peak pattern with standard, solubilised and plumbagin caged nanoparticles indicated the successful conjugation of plumbagin on silver nanoparticles. Supplementary fig 1 shows the photograph of plumbagin caged silver nanoparticles (PCSN) and control nanoparticles. The solubilised plumbagin from plumbagin caged on silver nanoparticles is provided in supplementary fig 2.

Fig. 2 (a, b) shows the SEM images of nanoparticles indicating uniform distribution of the nanoparticles in the ranges from 40-80nm. Negligible amount of aggregation was found in plumbagin caged nanoparticles when compared with control nanoparticles (without plumbagin). In order to reveal the presence of plumbagin on the silver nanoparticle, elemental analysis was performed along

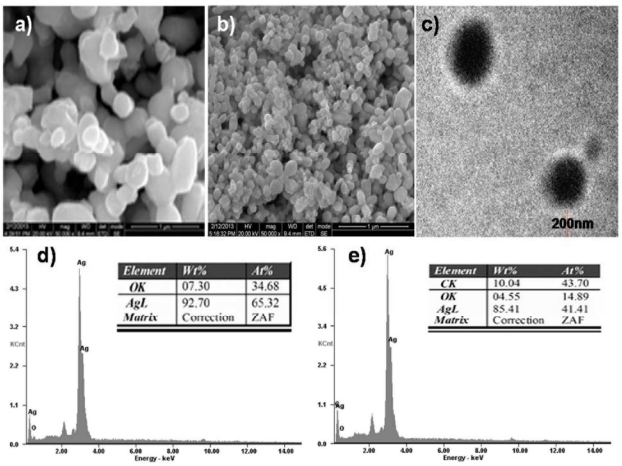

Fig.2 Electron microscopic analysis of plumbagin caged silver nanoparticle. a) Scanning electron microscopic images of control silver nanoparticle (without conjugation) and b) Scanning electron microscopic images of plumbagin caged nanoparticle. SEM images were captured at 50000X magnification. The SEM microphotograph shows that the average size and aggregation of plumbagin caged nanoparticles are less compared to the control silver nanoparticles c) Transmission electron microscopic images of plumbagin caged silver nanoparticle at 65000X magnification. The translucent area around the nanoparticles indicates the conjugation of plumbagin over silver nanoparticles d) EDS spectrum of control silver nanoparticle and e) EDS spectrum of plumbagin caged silver nanoparticle.

with SEM. EDS Spectrum is shown in Fig 2 (d, e). The appearance of carbon peak in the plumbagin caged silver nanoparticles when compared with the silver nanoparticles (Unconjugated) clearly indicated the conjugation of plumbagin on silver nanoparticle. The SEM EDS analysis thus confirmed the successful conjugation of plumbagin on silver nanoparticle. Fig.2c shows the TEM images of plumbagin caged silver nanoparticles. The TEM images further confirmed that the size and morphology of plumbagin caged nanoparticles in the range between 50 to 80 nm and the morphology was observed to be spherical. The area surrounding the nanoparticle was opaque owing to the uniform capping of plumbagin on the silver nanoparticles.

In vitro cyototoxicity of plumbagin caged silver nanoparticles:

The cell viability/toxicity of plumbagin caged silver nanoparticles was evaluated by the measuring the

mitochondrial dehydrogenases activity using MTT assay. HaCaT and A431 cells were treated with various concentrations of the plumbagin caged silver nanoparticle and unconjugated plumbagin for 24hrs and the activity of mitochondrial dehydrogenases was measured using MTT assay. The results are given in Fig.3. The results showed that the cell viability was app 90-100 % upto a concentration of 2.5 µM in normal cells (HaCaT) and the toxicity was observed only at concentration of plumbagin conjugated nanoparticle at or above 5 µM. On the other hand in cancerous cells (A431) nearly 95% was observed when treated with plumbagin caged nanoparticle at concentrations as low as 2.5µM.

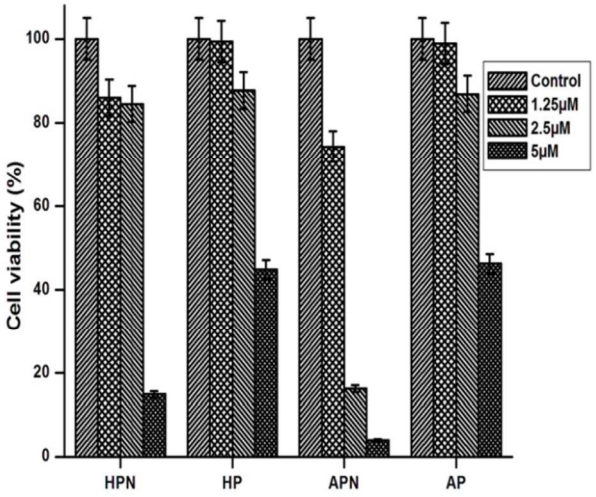

Fig.3 Biocompatibility of plumbagin caged silver nanoparticle. HaCaT and A431 cells were maintained DMEM medium containing plumbagin caged silver nanoparticle and plumbagin at varying concentrations of 1.25, 2.5 and 5 µM respectively for 24 hrs and cell viability was analysed using MTT assay. HPN- HaCaT cells treated against with plumbagin caged silver nanoparticles and HP with plumbagin. APN-A431 cells treated with plumbagin caged silver nanoparticle and AP with plumbagin.

The results showed that the cell viability was about 75%, 20% and 5% in A431 at the concentration ranges of 1.25, 2.5 and 5 µM respectively (concentration used was based on the solubilised amount of plumbagin from plumbagin caged silver nanoparticles) whereas in HaCaT cells the significant toxicity was observed only at 5 µM concentration. This indicated that the functionalized nanoparticle enhance the selective killing of cancer cell at concentration as low as 2.5 µM whereas the effect was not significant in concentrations above 5µM.

Effects of plumbagin caged silver nanoparticle on apoptosis:

In order to understand whether the cytotoxic effect observed with MTT assay is due to apoptosis, annexin propidium iodide staining for phosphatidyl serine externalization, a dual staining assay for apoptosis was performed. Fig 4 shows the microphotograph of HaCaT and A431 cells treated with plumbagin caged silver nanoparticle and unconjugated plumbagin. The results indicated that A431 and HaCaT cells treated with unconjugated plumbagin at concentration of 1.25, 2.5µM did not show any apoptotic features as indicated by no fluorescence on annexin propidium iodide staining whereas significant amount of apoptotic cells were observed in both A431 cells and HaCaT cells at 5 µM concentration. However significant difference in the apoptotic effect was observed in cells treated with plumbagin caged nanoparticles. Significant amount of late apoptotic cells were observed in A431 cells treated with 2.5 µM concentration of plumbagin caged nanoparticles, whereas no apoptotic cells were observed HaCaT cells at this concentration.

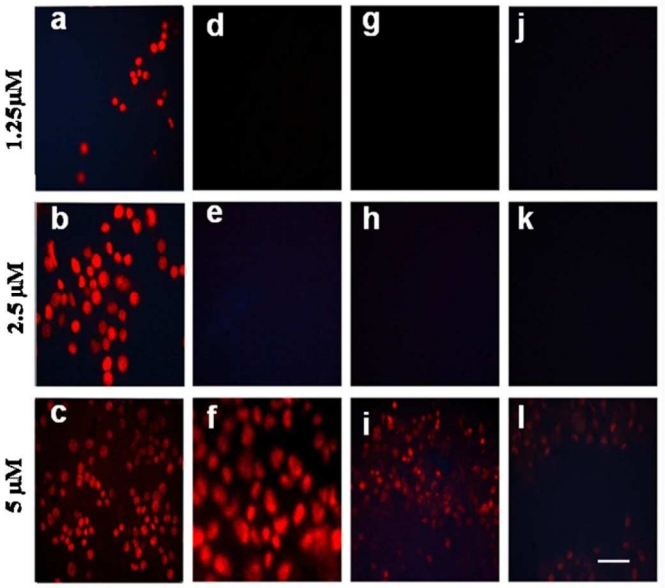

Fig.4 Apoptotic effect of plumbagin caged silver nanoparticle. HaCaT and A431 cells were treated with plumbagin caged nanoparticle and plumbagin at varying concentrations of 1.25, 2.5 and 5 µM respectively and the cells were stained with annexin/propidium iodide. A431 treated with plumbagin caged silver nanoparticles (a,b,c), and plumbagin (d, e,f), HaCaT treated with plumbagin caged silver nanoparticles (g, h, i) and plumbagin (j, k, l).Scale bar -10µm.

No significant apoptotic effect was observed in both HaCaT and A431 cells on treatment with plumbagin caged nanoparticles at concentration of 1.25 µM. The results are consistent with the MTT assay indicating a selective apoptosis on A431 cells at 2.5 µM concentration on treatment with plumbagin caged nanoparticles when compared with control cells. We quantitated the rate of apoptosis by FACS analysis and the results are provided in supplementary fig 3 and supplementary table 1. The data are consistent with MTT assay. We performed quantitation of apoptotic kinetic in A431 and HaCaT cells 6 hrs after treatment of plumbagin caged silver nanoparticle (PCSN) and plumbagin. The results showed significant apoptosis (18%) in cancerous A431 cells on treatment with 2.5 µM PCSN (PN1) whereas only 0.21 % apoptotic cells were observed in HaCaT and at 5 µM concentration only 50 % viability was observed in A431 cells whereas in HaCat cells showed more than 80 % cell viability. Further from the FACS data it is clear that at 5 µM concentration of PCSN significantly affects the cell viability as indicated by a decrease in the total cell population available for FACS measurement. It must be noted that the cell viability of HaCaT cells was 80% in all treated group including untreated control and about 18% cell was found Upper Left quadrant (UL) uniformly in all treatment group and untreated controls. Uniform distribution of 18% cells in UL quadrant in HaCaT cells in all treatment groups and untreated controls indicates that certain

amount of cell death is happening in HaCaT cells while processing for FACS analysis. If that is ignored we can assume that 100% viability for HaCaT cells. But such a phenomenon is not observed with A431 cells. This difference may be due to the difference in the sturdiness of the cells to overcome the processing steps while performing FACS analysis. Unconjugated plumbagin at same concentration had very little effect on A431 cells. We also observed very little apoptosis in normal HaCaT cells at all concentrations on treatment with plumbagin and plumbagin caged silver nanoparticles. The results indicated that PCSN caused a selective targeted killing of cancerous cell when compared to normal cells.

Cell viability and apoptotic assay was performed with control nanoparticles having similar size (compared to PCSN, 50-80nm) with concentrations corresponding to 1.25µM, 2.5 µM and 5 µM concentration of PCSN. The results showed that silver nanoparticles did not exhibit any toxicity at. The study therefore confirms that the conjugation alone induces selectivity and sensitivity (not toxicity) to plumbagin therapy since control silver nanoparticles at concentrations where PCSN showed selectivity (2.5 µM) had 90% above viability in both HaCaT and A431 cells and no apoptotic cells were viable after annexin propidium iodide staining. The results are provided in supplementary fig 4 and 5. Control nanoparticles having similar size corresponding to PCSN were synthesised by citrate reduction in presence of ascorbic acid following the procedure describe earlier by Qin and co-workers[25].

Mitochondrial mediated apoptosis through plumbagin caged silver nanoparticles:

The mechanism of apoptosis induced by plumbagin caged silver nanoparticle was further analysed by measuring the activity of caspase 3 and 9 on A431 and HaCaT cells. Fig. 5 shows the activation level of caspase 3 and 9.

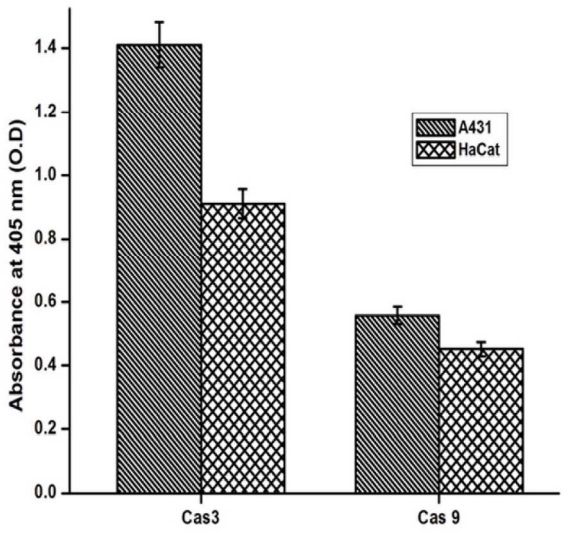

Fig.5 Effect of plumbagin caged silver nanoparticle on caspase activity. HaCaT and A431 cells were treated with plumbagin caged silver nanoparticle and plumbagin at varying concentrations of 1.25, 2.5 and 5 µM respectively. The activation levels of caspase-3 and 9 was analysed and expressed as OD units/mg protein.

Caspase 9 activity was similar in both HaCaT and A431 cells on treatment with plumbagin caged silver nanoparticles. But significant caspase 3 activation was observed in A431 cells on treatment with plumbagin caged nanoparticles when compared with HaCaT cells. A significant increase in the activation of caspase 3 was observed in A431 cells in comparison with HaCaT cells. The results indicated that plumbagin caged silver nanoparticles induced cell death via caspase 3 dependent apoptotic pathway.

Intracellular ROS role in apoptosis and mitochondrial respiratory chain:

It has been reported that plumbagin mediated cell death and toxicity by in situ ROS generation. We analyzed the ROS levels using molecular probe 2, 7 dichloro dihydrofluorescin diacetate (DCFH-DA). Fig.6a shows the ROS levels in A431 and HaCaT cells on treatment with various concentrations (1.25, 2.5 and 5µM) of plumbagin and plumbagin caged silver nanoparticles. The green fluorescence intensity indicative of ROS levels in A431 and HaCaT cells increased in a concentration dependent manner for both plumbagin (Unconjugated) and plumbagin caged silver nanoparticles. The ROS generation as indicated by green fluorescence intensity from the HaCaT cells was significantly low at 1.25 and 2.5 µM concentrations on treatment with both plumbagin and plumbagin caged silver nanoparticles where as significant fluorescence was observed from HaCaT cells at 5 µM concentrations. In the case of A431 cells significant ROS generation was observed at 2.5 µM concentrations on treatment with plumbagin caged silver nanoparticles whereas in unconjugated plumbagin treated A431cells ROS generation was observed only at concentration of 5µM.

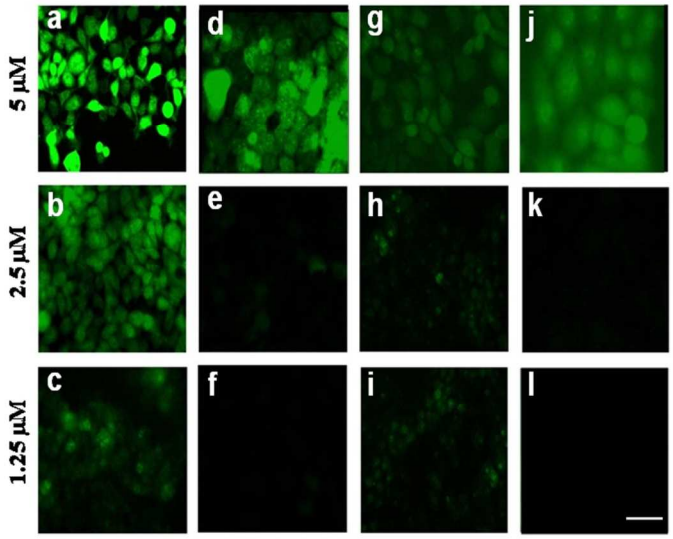

Fig.6 a) Detection of intracellular ROS levels in HaCaT and A431 cells. HaCaT and A431 cells were treated with plumbagin caged nanoparticle and plumbagin at varying concentrations of 1.25, 2.5 and 5 µM. The cells were treated with DCFH-DA and the microphotograph captured using a Leica fluorescent microscope. A431 treated with plumbagin caged silver nanoparticles (a, b, c) and Plumbagin (d, e, and f). HaCaT treated with plumbagin caged silver nanoparticles (g, h, i), and plumbagin (j, k, l). Scale bar 10µm.

The results indicated that the biological effect mediated by plumbagin caged nanoparticles was observed to be through ROS generation similar to that observed for plumbagin however conjugation of plumbagin with silver nanoparticles selectively seems to lower the effective concentration to bring about the biological effect. In order to study whether the apoptotic effects mediated by plumbagin caged silver nanoparticles is mediated through the ROS generation we

analysed the effect of cell viability in presence of anti-oxidant vitamin C. The results are given in Fig 6b.

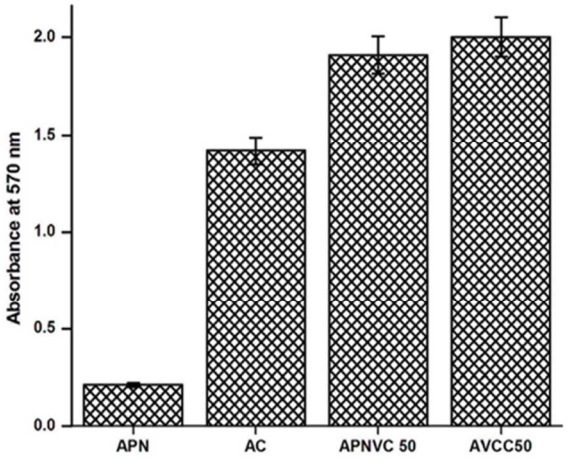

Fig.6. b) Effect of antioxidants on bioactivity of plumbagin caged silver nanoparticles. A431 cells treated with plumbagin caged silver nanoparticle (2.5 µM) and vitamin C (50µM) was incubated for 24 hrs. The cell viability was analyzed by using MTT assay. APN-A431 treated with plumbagin caged nanoparticle and AC-A431 control. APNVC50-APN-A431 treated with plumbagin caged nanoparticle along with vitamin C (50 µM) and AVCC50 with vitamin C (50 µM).

The results showed that treatment with vitamin C (50µM) completely revised cytotoxic effect induced by plumbagin caged silver nanoparticles. The cell viability was 100% when compared with untreated control cells indicated that the quenching of ROS challenge can revise the cytotoxic effect of plumbagin caged silver nanoparticles.

Effect of plumbagin caged silver nanoparticles on pyruvate kinase activity:

We further analysed the mechanism of action of plumbagin caged silver nanoparticles on cancerous cells. It has been reported that the levels of intracellular ROS is critical for cancer cell survival. Pyruvate kinase (PK) is the glycolytic enzyme which has critical role in cancerous cell metabolism under redox challenge. In order to understand the effect of plumbagin caged silver nanoparticles on pyruvate kinase activity we treated A431 cells and HaCaT cells with plumbagin caged silver nanoparticles and analysed the pyruvate kinase activity. The results are shown in Fig. 7.

The results indicated that the amount of pyruvate kinase activity in A431 cells treated with plumbagin caged silver nanoparticles was significantly increased compare with HaCaT cells. A significant increase in the activity was observed in A431 cells treated with plumbagin caged silver nanoparticles compared with untreated controls. Further the activity of pyruvate kinase was also increased in A431cells treated with plumbagin at same concentration (2.5µM) alone when compared to control although the increase was not significantly higher. No increase in PK activity was observed at 2.5µM concentration of plumbagin caged silver nanoparticle and plumbagin (Unconjugated) in HaCaT cells when compared with the untreated controls.

In this manuscript we demonstrated the effect of caging of plumbagin on silver nanoparticle on the biochemical activities of plumbagin. We observed that conjugation of plumbagin with silver nanoparticle decreased the effective concentration to induce cell toxicity in cancerous cells when compared with the unconjugated plumbagin. Further, caging of plumbagin on silver nanoparticles imparted selectivity and sensitivity of cytotoxic/apoptotic effects towards the cancerous cells. We observed that the caging of plumbagin on silver nanoparticle induce cytotoxicity (80% cell death) in A431 cell at 2.5µM when compared with HaCaT cells where plumbagin caged silver nanoparticles induced significant cytotoxic effect only at 5µM concentration. Unconjugated plumbagin affected the viability of both cancerous cells and normal cells at 5µM concentration and concentrations below 5 µM had no significant effect on the viability of both cancerous and normal cells line. Similar results were also observed with other cell lines namely NIH3T3 and MG63 cells where at concentration of 2.5µM PCSN induced significant toxicity in MG63 cells whereas the cell viability of NIH3T3 cells were not affected (data not shown).

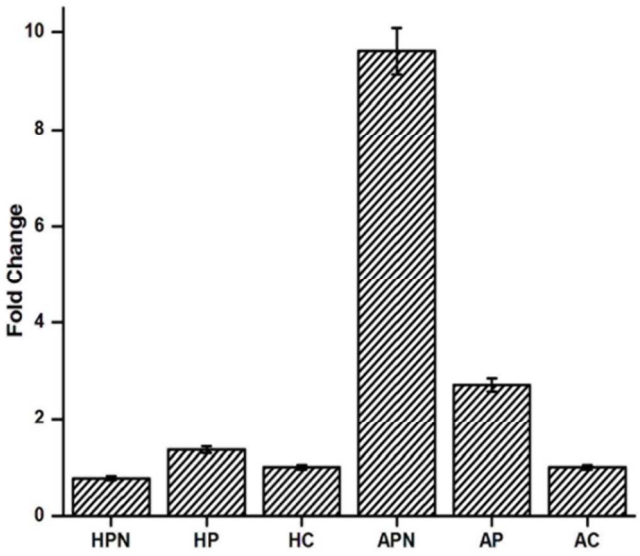

Fig.7 Effect of plumbagin caged silver nanoparticle on pyruvate kinase activity. The activity level is expressed as fold change normalized with untreated control cells. HPN-HaCaT cells treated with plumbagin caged silver nanoparticles and plumbagin HP. HC-Untreated control. APN-A431 cells treated with plumbagin caged silver nanoparticles and plumbagin AP. AC- Untreated control

It has been reported that plumbagin induces cytotoxic effect via apoptosis through generation of free radicals.[26-28] We observed that the conjugation of plumbagin did not affect its ROS mediated mechanism through which cell death or cytotoxic effect is initiated.[29] Similar to plumbagin, plumbagin caged silver nanoparticle also induces apoptosis via caspase 3 dependent pathway through ROS generations[30,31]. The apoptotic effect seems to be concentration and cell type dependent. Apoptosis was observed to be significant in A431 cells at 2.5µM concentration whereas no significant apoptosis was observed at and below 2.5µM concentration. In HaCaT cells, apoptosis was only observed at 5 µM concentrations and no significant apoptosis was observed at concentrations below 5µM. The results suggest that the selectivity and sensitivity of plumbagin towards A431 cells may be due to its caging on silver nanoparticle. It seems that the cumulative properties of plumbagin and silver nanoparticle impart selectivity and sensitivity against cancer cell.

Silver nanoparticles have been reported to exhibit several assorted pharmacological effects namely anti-inflammatory, [32-35] wound repair, [36, 37] and anti-angiogenic activity[38]. It has been reported that silver nanoparticle generates ROS to mediate the biological effects.[39-41] On the other hand plumbagin has been reported to have much similar biological effect like that of silver nanoparticles.[42, 43] Many of the biological effects have been reported to be due to the ROS generation that indicates that combination of silver nanoparticles and plumbagin would have cumulative effect on the biological activities they possess. The effect of selectivity and sensitivity seems to be due to the cumulative effects of the plumbagin and silver nanoparticles, since no such effects was observed when cells were treated with individual molecules. We assume that the cumulative properties of plumbagin and silver nanoparticles would aide in reducing the effective concentrations of each molecule to bring about the biological effects.

The selectivity and sensitivity of plumbagin caged nanoparticle on cancerous cells may be due to the difference in the microenvironment of the cancerous cells and normal cells. Cancer cells are under constant ROS challenge due to the continuous respiration to support uncontrolled cell division. Pyruvate kinase is glycolytic, rate limiting enzyme which determines the rate of metabolism of cell by its dual action. It participates in the final step of glycolysis in the conversion of phospho enol pyruvate (PEP) into pyuvate or it can also shunt PEP for serine biosynthesis or pentose phosphate pathway to generate ribose and NADPH to promote cell proliferation via anabolic process called aerobic glycolysis.[44, 45] The activity of this enzyme to utilize PEP for pyruvate formation or pentose phosphate pathways depends on the concentration of this enzyme available in the microenvironment. At low levels this enzyme shunts PEP for pentose phosphate pathways and at high concentrations it promotes the synthesis of pyruvate from PEP.[46] The regulation of intracellular ROS concentrations is critical for cancer cell survival. Cancer cells are under constant ROS challenge since the conditions associated with cancer progression such as matrix detachment, inflammation, hypoxia and mitochondria dysfunction all results in ROS generation. PKM2 may confer advantage to cancer cells by allowing them to withstand oxidative stress. In cancer cells, increases in intracellular concentrations of ROS results in the inhibition of the glycolytic enzyme pyruvate kinase M2 (PKM2). This inhibition of PKM2 results in diversion of glucose flux into the pentose phosphate pathway and thereby generates sufficient reducing potential for detoxification of ROS. Cancer cells expressing PKM2 mutant where the Cys (358) was changed with Ser (358) exhibited increased sensitivity to ROS and inhibited the tumour formation in a xenograft model indicating that alteration in the regulation of PKM2 activity can affect the cancer cell survival.[47]

Our study is consistent with the above reports that showed that treatment with plumbagin caged silver complex results in the increased activity of PK. The feedback mechanisms that regulate the PK activity to produce antioxidants seem to be affected. Increased activity of PK results in fluxing the metabolite to glycolytic pathways that may induce the generation of intracellular ROS. However no such effect was observed in control cells. It has been reported that excess ROS may assist the aerobic respiration in cancerous cell.[48] Luo et al (2011) reported that the increased rate of pyruvate kinase activity is caused by the expression of hypoxia inducible factor-1 in cancer cell.[49] Interestingly, we assume that the acute increase in the ROS due to the treatment of plumbagin caged silver nanoparticles would result in over activation of HIF-1 that in turn increases PKM2 activity. Thus the total ROS in the cancer cell microenvironment would increase significantly high enough to be controlled by the regulatory mechanism that regulate ROS levels, finally this would results in apoptosis of cells. Excessive levels of ROS has been reported to increase the PKM2 levels that results in the translocation of this enzyme along with beta catenin into the nucleus and activate caspase gene expression leading to cell apoptosis.[50] The apoptosis and the cytotoxicity induced on cancerous cell line A431 on treatment with 2.5µM plumbagin caged silver nanoparticles would be due to the excessive generation of ROS imparted by the cumulative effect of plumbagin and silver nanoparticles in addition to the already persisting ROS challenge in cancer cell microenvironment that results in activation of caspases leading to apoptosis. The mechanism of action of plumbagin caged silver nanoparticles on cancerous cells is schematically represented in Fig 8.

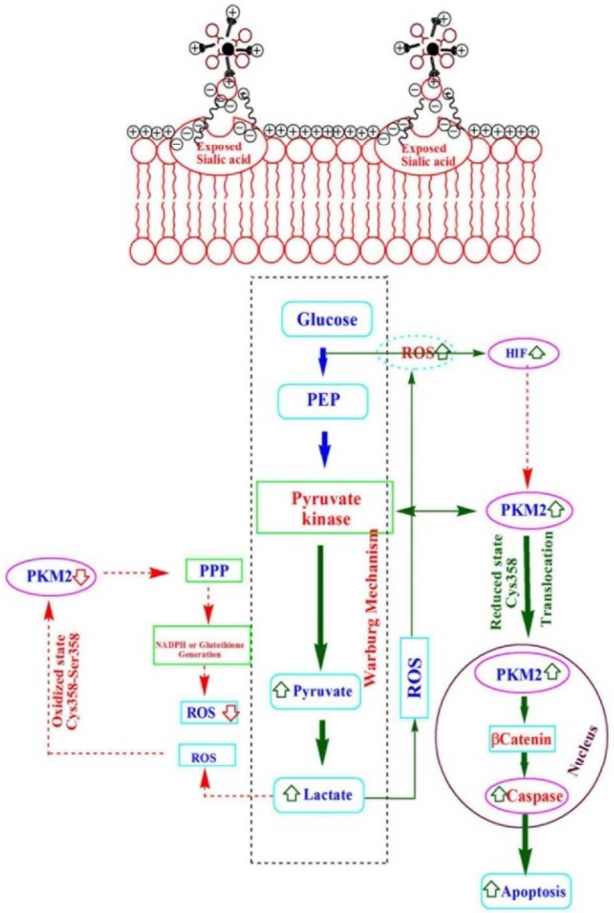

Fig.8 Schematic representation of mechanism of action of plumbagin caged silver nanoparticles on cancerous cells.

Furthermore the charge difference between the cell and the nanoparticles would play major role in the biochemical activities of nanoparticles. There are many reports suggested that the cellular uptake of nanoparticle due to the surface charge of the cancerous cells.[51]Mostly all cancerous cells are anionic due to the exposed terminal carboxyl group of sialic acid residues in the cells and the silver nanoparticles are positively charged which makes them attracted towards cancerous cells bringing in selectivity of these nanoparticles towards cancerous

cells sparing the normal cells[52-56]. We observed that control nanoparticles have a surface charge of -23 and PCSN showed a surface charge of +0.4 indicating that caging of plumbagin on silver nanoparticle changes its surface chemistry and brings the potential to the positive side compared to the unconjugated control nanoparticles (Supplementary fig 6). We assume that such selective cytotoxicity toward cancerous cells would be because of the interaction of plumbagin caged nanoparticle with the cancerous cell due to the differences in surface chemistry of PCSN when compared with control nanoparticles. Further this interaction would facilitate the localized availability of plumbagin caged on silver nanoparticles to bring about apoptosis in cancerous cells.

Conclusions

Plumbagin caged silver nanoparticles imparted sensitivity and selectivity to plumbagin for cancer cell apoptosis. The cumulative effects of both the conjugated nanoparticles and plumbagin resulted in bringing the sensitivity and selectivity towards cancers cells apoptosis. Further we observed that the plumbagin caged silver nanoparticles induced approximately 80% cell death concentrations as low as 2.5µM whereas no cytotoxicity was observed in normal cells. These results indicated that the nano-biotechnological approach added therapeutic values to plumbagin for its application as anti-cancer drug.

Acknowledgements

We thank Dr. Asit Baran Mandal, Director, and CSIR-CLRI for providing the infrastructure to carry out this research work. The first author acknowledges INSPIRE PROGRAMME, Department of Science and Technology, Government of India for the financial support in the form of DST JRF (IF120634). The work was supported by DBT, Government of India (RGYI grant, GAP 1062) and CSIR, Government of India (NanoSHE, BSC0112).

Notes and references

[a] Council of Scientific and Industrial Research-CLRI, Chennai-20

[b] Academy of Scientific and Innovative Research, New Delhi, India

*E-mail: kiranmsk112@gmail.com, kiran@clri.res.in

Electronic Supplementary Information (ESI) available:

[**Supplementary Fig 1** Synthesis of plumbagin caged silver nanoparticles. Photographic representation of a) Silver nitrate solution alone b) Silver oxide nanoparticles (reduced with KOH) and c) Plumbagin caged silver nanoparticles.

Supplementary Fig 2 Caging efficiency of plumbagin on silver nanoparticles was determined after solubilization in alcoholic KOH. a) Supernatant from control nanoparticles after treatment with alcoholic KOH b) Supernatant from plumbagin caged silver nanoparticles after treatment with alcoholic KOH. The supernatant was used to quantitate the plumbagin loading efficiency on silver nanoparticles using UV-Vis Spectroscopy and FT-IR analysis

Supplementary Fig 3 Flow cytometric quantification of apoptosis induced by plumbagin and plumabagin caged silver nanoparticle. HaCaT and A431 cells were treated with plumbagin caged silver nanoparticle and plumbagin at 2.5 µM and 5 µM concentrations and incubated for 6 hrs at 37ºC. The cells were then stained with Annexin-FITC and PI for 30 mins at dark and the cells were harvested and quantified using flow cytometer (BD Bioscience). P1, P2 illustrated the A431 and HaCaT treated with 2.5 µM and 5 µM of plumbagin concentration respectively. PN1 and PN2 illustrated that the both cells A431 and HaCaT treated with 2.5 µM and 5 µM concentration of plumbagin caged silver nanoparticle respectively.

Supplementary Fig 4 a) Dynamic light scattering analysis of the control silver nanoparticle synthesised by citrate reduction method in presence of ascorbic acid. **b)** Scanning electron microphotograph of control silver nanoparticle. **c)** Effect of control silver nanoparticle having size similar to PCSN on cell viability of A431 and HaCaT cells; A- untreated control, B, C, and D represents the concentrations corresponding to 1.25 µM, 2.5 µM, 5 µM PCSN respectively.

Supplementary Fig 5 Effect of control silver nanoparticle having size similar to PCSN on Apoptosis: A, B and C represents the concentrations of control nanoparticle corresponding 1.25 µM, 2.5 µM, 5 µM of PCSN. a, b, c – Phase contrast images of A431 cells; d, e, f – Fluorescence images of A431 cells. g, h, i – Phase contrast images of HaCaT cells; j, k, l – Fluorescent images of HaCaT cells.

Supplementary Fig 6 Zeta Potential measurement of **a)** Control silver nanoparticle. **b)** PCSN nanoparticle.

Supplementary Table 1 Flow cytometric quantification of apoptotic and viable cells on treatment with plumbagin and plumabagin caged silver nanoparticle. P1, P2 represents the A431 and HaCaT cells treated with 2.5 µM and 5 µM concentration of plumbagin respectively. PN1 and PN2 illustrated that the both A431 and HaCaT cells treated with 2.5 µM and 5 µM concentration of plumbagin caged silver nanoparticle respectively]. See DOI: 10.1039/b000000x/

References

1 S.C. Gupta, J.H. Kim, S. Prasad and B.B. Aggarwal, *Cancer Metastasis Rev*., 2010, **29**, 405-34.

2 M. Hamburger and K. Hostettmann, *Phytochemistry*, 1991, **30**, 3864–3874.

3 O.R. Gottlieb, M. R Borin, and N.R. de Brito, *Phytochemistry*, 2002, **60**, 145-52.

4 G. Santhakumari, P.G. Saralamma and N. Radhakrishnan, *Indian J Exp Biol,* 1980, **18**, 215-8

5 S.B. Farr, D.O. Natvig, and T. Kogoma, *J Bacteriol*, 1985,**164**, 1309-16.

6 J.J. Inbaraj and C.F. Chignell, *Chem. Res. Toxicol*., 2004, **17**, 55-62.

7 S. Padhye, P. Dandawate, M. Yusufi, A. Ahmad and F.H. Sarkar*, Med. Res. Rev*., 2012, **32**, 1131-58.

8 L. M. Van der Vijver, *Phytochemistry*, 1972, **11**, 3247– 3248.

9 J. S. Mossa, F.S. El-Feraly and I.Muhammad, *Phytother. Res*., 2004, **18**,934-7.

10 Y. Ding, Z. J. Chen, S. Liu, D. Che, M. Vetter and C.H. Chang, *J. Pharm. Pharmacol*., 2005, **57**, 111-6.

11 Y.J. Hsieh, L.C. Lin, and T.H. Tsai, *J. Chromatogr. A*, 2005, **1083**, 141-5.

12 U.V. Singh and N. Udupa, *Indian J. Physiol. Pharmacol*., 1997, **41**,171-5.

13 A.L. Martin, B. Li and E.R. Gillies, *J. Am. Chem. Soc*., 2009, **131**, 734-41.

14 A. Quarta, R. Di Corato, L. Manna, S. Argentiere, R. Cingolani, G. Barbarella and T. Pellegrino, *J. Am. Chem. Soc.,* 2008, **130**:10545-55.

15 X. Li, J. Guo, J. Asong, M.A. Wolfert, and G.J. Boons, *J. Am. Chem. Soc*., 2011, **133**, 11147-53.
16 R. A. Sperling and W. J. Parak, *Philos. Trans. A. Math. Phys. Eng. Sci.,* 2010, **368**, 1333-83.
17 K. Kesarwani, R. Gupta and A. Mukerjee, *Asian Pac. J. Trop. Biomed.*, 2013, **3**, 253-66.
18 L. Vigderman, and E.R. Zubarev, *Adv. Drug Deliv. Rev.*, 2013, **65**, 663-76.
19 R. Gref, P. Couvreur, G. Barratt and E. Mysiakine, *Biomaterials,* 2003, **24**, 4529-37.
20 T. Hanemann and D.V. Szabo, *Materials,* 2010, **3**, 3468-517.
21 D. L. Leslie-Pelecky in Biomedical Applications of Nanotechnology. ed. V. Labhasetwar and, D.L. Leslie-Pelecky, Wiley-interscience, A john wiley & son, inc., publication. Hoboken, New Jersey, 2007, pp. 227-241.
22 T. Mosmann, *J. Immunol. Methods,* 1983, **65**, 55-63.
23 A. Aranda, L. Sequedo, L. Tolosa, G. Quintas, E. Burello, J. V. Castell and L. Gombau, *Toxicol. In Vitro,* 2013, **27,** 954-63.
24 H. R. Christofk, M. G. Vander Heiden, M. H. Harris, A. Ramanathan, R. E. Gerszten, R. Wei, M. D. Fleming, S. L. Schreiber and L. C. Cantley, *Nature,* 2008, **452**, 230-3.
25 Y. Qin, X. Ji, J. Jing, H. Liu, H. Wu, and W. Yang, *Colloids Surf. A Physicochem. Eng. Aspects,* 2010, **372,** 172–6.
26 P. Srinivas, G. Gopinath, A. Banerji, A. Dinakar and G Srinivas. *Mol. Carcinog*., 2004, **40**, 201-11.
27 S. K. Sandur, H. Ichikawa, G. Sethi, K. S. Ahn and B. B Aggarwal, *J. Biol. Chem.,* 2006, **281**, 17023-33.
28 K. H. Xu and D. P. Lu, *Leuk. Res*., 2010, **34,** 658-65.
29 P. Srinivas, C. R. Patra, S. Bhattacharya and D. Mukhopadhyay, *Int. J. Nanomedicine*., 2011, **6**, 2113-22.
30 J. Wang and M. J. Lenardo, *J. Cell. Sci.,* 2000, **113**, 753-7.
31 P. Seshadri, A. Rajaram and R. Rajaram, *Free Radic. Biol. Med.,* 2011, **51**, 2090-107.
32 R. E. Burrell, J. P. Heggers, G. J. Davis and J. B. Wright, *Wounds*, 1999, **11**, 64-71.
33 S. W. P. Wijnhoven, W. J. G. M. Peijnenburg, C. A. Herberts, W. I. Hagens, A. G. Oomen, E. H. W. Heugens, B. Roszek, J. Bisschops, I. Gosens, D. van de Meent, Dekkers S, W. H. De Jong, M. Van zijverden, A. J. A. M. Sips and R. E. Geertsma, *Nanotoxicol.,* 2009, **3**, 109–138.
34 P. L. Nadworny, J. Wang, E. E. Tredget and R. E. Burrell, *Nanomedicine,* 2008, **4,** 241-51.
35 (34) P. L. Nadworny, B. K. Landry, J. Wang, E. E. Tredget and R. E. Burrell, *Wound Repair Regen.*, 2010, **18**, 254-65.
36 R. S. Kirsner, H. Orstead and J. B. Wright, *Wounds*, 2001, **13**: 5–12.
37 J. Tian, K. K. Wong, C. M. Ho, C. N. Lok, W. Y. Yu, C. M. Che, J. F. Chiu and P. K. Tam, *Chem. Med. Chem*., 2007, **2**, 129-36.
38 S. Gurunathan, K. J. Lee, K. Kalishwaralal, S. Sheikpranbabu, R. Vaidyanathan and S. H. Eom, *Biomaterials,* 2009, **30,** 6341-50.
39 Y. H. Hsin, C. F. Chen, S. Huang, T. S. Shih, P. S. Lai and P. J. Chueh, *Toxicol. Lett.,* 2008, **179**,130-9.
40 S. Hackenberg, A. Scherzed, M. Kessler, S. Hummel, A. Technau, K. Froelich, C. Ginzkey, C. Koehler, R. Hagen and N. Kleinsasser, *Toxicol. Lett.,* 2011, **201**, 27-33.
41 Y. H. Su, Z. F. Yin, H. L. Xin, H. Q. Zhang, J. Y. Sheng, Y. L. Yang, J. Du and C. Q. Ling, *Int. J. Nanomedicine*, 2011, **6,** 1579-86.
42 Y. L. Hsu, C. Y. Cho, P. L. Kuo, Y. T. Huang and C. C. Lin, *J. Pharmacol. Exp. Ther.*, 2006, **318**, 484-94.
43 F. A. Castro, D. Mariani, A. D. Panek, E. C. Eleutherio and M. D. Pereira. *PLoS One*, 2008, **3**, e3999.
44 M. A. Iqbal, F. A. Siddiqui, V. Gupta, S. Chattopadhyay, P. Gopinath, B. Kumar, S. Manvati, N. Chaman and R. N. Bamezai, *Mol. Cancer*, 2013, **12**, 72
45 H. P. Morgan, F. J. O'Reilly, M. A. Wear, J. R. O'Neill, L. A. Fothergill-Gilmore, T. Hupp and M. D. Walkinshaw, *Proc. Natl. Acad. Sci. U S A,* 2013, **110**, 5881-6.
46 R. B. Hamanaka and N. S. Chandel, *Science*, 2011, **334,** 1219-20.
47 D. Anastasiou, G. Poulogiannis, J. M. Asara, M. B. Boxer, J. K. Jiang, M. Shen, G. Bellinger, A. T. Sasaki, J. W. Locasale, D. S. Auld, C. J. Thomas, M. G. Vander Heiden and L. C. Cantley, *Science*, 2011, **334**, 1278-83,
48 F. Weinberg, R. Hamanaka, W. W. Wheaton, S. Weinberg, J. Joseph, M. Lopez, B. Kalyanaraman, G. M. Mutlu, G. R. Budinger and N. S. Chandel, *Proc. Natl. Acad. Sci. U S A,* 2010, **107**, 8788-93.
49 W. Luo and G. L. Semenza. *Oncotarget*, 2011, **2**, 551-6.
50 A. Stetak, R. Veress, J. Ovádi, P. Csermely, G. Kéri and A. Ullrich, *Cancer Res.,* 2007, **67**, 1602-8.
51 D. van Lierop, Z. Krpetic, L. Guerrini, I. A. Larmour, J. A. Dougan, K. Faulds and D. Graham, *Chem. Commun. (Camb),* 2012, **48**, 8192-4.
52 M. Marquez, S. Nilsson, L. Lennartsson, Z. Liu, T. Tammela, M. Raitanen and A. R. Holmberg, *Anticancer Res.,* 2004, **24**, 1347-51.
53 E. Caballero-Diaz, C. Pfeiffer, L. Kastl , P. Rivera-Gil, B. Simonet , M. Valcarcel, J. Jimenez-Lamana , F. Laborda and W.J. Parak, *Part. Part. Syst. Charact.,* 2013, **30,** 1079–85.
54 A.K. Suresh, D. Pelletier, W. Wang, J.L. Morrell-Falvey, B. Gu and M.J. Doktycz, *Langmuir*, 2012, **28,** 2727–35.

55 B. Reidy, A. Haase, A. Luch, K.A. Dawson, I. Lynch, *Materials,* 2013, **6,** 2295-350.
56 Z. Sui, X. Chen, L. Wang, Y. Chai, C. Yang, J. Zhao. *Chemistry Lett.,* 2005, **34,** 100-1.

Legends to Figures

Fig.1 Characterization of plumbagin caged silver nanoparticles a) UV-visible spectrum of plumbagin caged silver nanoparticles b) Particle size analysis of plumbagin caged silver nanoparticles. c) XRD pattern of plumbagin caged silver nanoparticles. d) FTIR spectra of Plumbagin (A), Plumbagin solublised from plumbagin caged silver nanoparticles (B), plumbagin caged silver nanoparticles (C). The FTIR spectrum shows conjugation of plumbagin on silver nanoparticles as indicated by similar FTIR patterns for plumbagin in all the samples analyzed.

Fig.2 Electron microscopic analysis of plumbagin caged silver nanoparticle. a) Scanning electron microscopic images of control silver nanoparticle (without conjugation) and b) Scanning electron microscopic images of plumbagin caged nanoparticle. SEM images were captured at 50000X magnification. The SEM microphotograph shows that the average size and aggregation of plumbagin caged nanoparticles are less compared to the control silver nanoparticles c) Transmission electron microscopic images of plumbagin caged silver nanoparticle at 65000X magnification. The translucent area around the nanoparticles indicates the conjugation of plumbagin over silver nanoparticles d) EDS spectrum of control silver nanoparticle and e) EDS spectrum of plumbagin caged silver nanoparticle.

Fig.3 Biocompatibility of plumbagin caged silver nanoparticle. HaCaT and A431 cells were maintained DMEM medium containing plumbagin caged silver nanoparticle and plumbagin at varying concentrations of 1.25, 2.5 and 5 µM respectively for 24 hrs and cell viability was analysed using MTT assay. HPN- HaCaT cells treated against with plumbagin caged silver nanoparticles and HP with plumbagin. APN-A431 cells treated with plumbagin caged silver nanoparticle and AP with plumbagin.

Fig.4 Apoptotic effect of plumbagin caged silver nanoparticle. HaCaT and A431 cells were treated with plumbagin caged nanoparticle and plumbagin at varying concentrations of 1.25, 2.5 and 5 µM respectively and the cells were stained with annexin/propidium iodide. A431 treated with plumbagin caged silver nanoparticles (a,b,c), and plumbagin (d, e,f), HaCaT treated with plumbagin caged silver nanoparticles (g, h, i) and plumbagin (j, k,l). Scale bar represents 10 µm.

Fig.5 Effect of plumbagin caged silver nanoparticle on caspase activity. HaCaT and A431 cells were treated with plumbagin caged silver nanoparticle and plumbagin at varying concentrations of 1.25, 2.5 and 5 µM respectively. The activation levels of caspase-3 and 9 was analysed and expressed as OD units/mg protein.

Fig.6a Detection of intracellular ROS levels in HaCaT and A431 cells. HaCaT and A431 cells were treated with plumbagin caged nanoparticle and plumbagin at varying concentrations of 1.25, 2.5 and 5 µM. The cells were treated with DCFH-DA and microphotograph captured using a Leica fluorescent microscope. A431 treated with plumbagin caged silver nanoparticles (a, b, c) and plumbagin (d, e, and f). HaCaT treated with plumbagin caged silver nanoparticles (g, h, i), and plumbagin (j, k, l). Scale bar 10µm**.**

Fig.6b Effect of antioxidants on bioactivity of plumbagin caged silver nanoparticles. A431 cells treated with plumbagin caged silver nanoparticle (2.5 µM) and vitamin C (50µM) was incubated for 24 hrs. The cell viability was analyzed by using MTT assay. APN-A431 treated with plumbagin caged nanoparticle and AC-A431 control. APNVC50-APN-A431 treated with plumbagin caged nanoparticle along with vitamin C (50 µM) and AVCC50 with vitamin C (50 µM).

Fig.7 Effect of plumbagin caged silver nanoparticle on pyruvate kinase activity. The activity level is expressed as fold change normalized with untreated control cells. HPN-HaCaT cells treated with plumbagin caged silver nanoparticles and plumbagin HP. HC-Untreated control. APN-A431 cells treated with plumbagin caged silver nanoparticles and plumbagin AP. AC- Untreated control.

Fig.8 Schematic representation of mechanism of action of plumabgin caged silver nanoparticles on cancerous cells.

